

To See or To Please: Uncovering Visual Sycophancy and Split Beliefs in VLMs

Rui Hong^{*1} and Shuxue Quan²

¹ George Mason University, Fairfax, VA, USA

² Independent Researcher

Abstract. When VLMs answer correctly, do they genuinely rely on visual information or exploit language shortcuts? We introduce the **Tri-Layer Diagnostic Framework**, which disentangles hallucination sources via three metrics: *Latent Anomaly Detection* (perceptual awareness), *Visual Necessity Score* (visual dependency, measured via KL divergence), and *Competition Score* (conflict between visual grounding and instruction following). Using counterfactual interventions (blind, noise, and conflict images) across 7 VLMs and 7,000 model-sample pairs, our taxonomy reveals that **69.6%** of samples exhibit *Visual Sycophancy*—models detect visual anomalies but hallucinate to satisfy user expectations—while **zero samples** show *Robust Refusal*, indicating alignment training has systematically suppressed truthful uncertainty acknowledgment. A scaling analysis (Qwen2.5-VL 7B→72B) shows larger models reduce Language Shortcuts but amplify Visual Sycophancy, demonstrating scale alone cannot resolve the grounding problem. Diagnostic scores further enable a post-hoc selective prediction strategy achieving up to +9.5pp accuracy at 50% coverage with no additional training cost.

Keywords: Vision-Language Models · Hallucination · Visual Sycophancy · Diagnostic Framework · Selective Prediction

1 Introduction

Vision-Language Models (VLMs) have demonstrated impressive capabilities across diverse multimodal tasks, from visual question answering to image captioning and reasoning. Recent state-of-the-art models such as Llama-3.2-11B [21] and Qwen2.5-VL [25] represent significant architectural advances and achieve high accuracy on standard benchmarks. However, despite these performance gains, growing evidence challenges whether these models genuinely process visual information.

Recent studies reveal a troubling paradox: VLMs often succeed *without genuinely utilizing visual information*. [29] show that state-of-the-art systems struggle with straightforward visual patterns, while [35] and [26] demonstrate failures on elementary compositional and low-level tasks. More strikingly, [6] and [8] reveal that removing images can maintain or even improve accuracy—suggesting visual input may act as a distractor.

^{*} Corresponding author: rhong5@gmu.edu

The Diagnostic Gap. These findings point to a fundamental limitation in current evaluation protocols: Accuracy alone cannot diagnose the root cause of grounding failures. When a VLM hallucinates or ignores visual data, accuracy metrics treat it as a binary error, masking the internal mechanism. Is the model suffering from *Perceptual Blindness* (the encoder cannot see the image)? Is it a *Language Shortcut* failure (the model ignores the visual tokens)? Or is it *Visual Sycophancy* (the model sees the truth but lies to satisfy user instruction)? Without distinguishing these mechanisms, we cannot effectively debug model behavior or mitigate hallucinations.

Our Approach. To bridge this gap, we propose the Tri-Layer Hallucination Diagnostic Framework. Instead of treating VLM generation as a black box, we dissect the decision-making process into three cognitive layers: **Perception**, **Dependency**, and **Alignment**. We introduce a causal intervention protocol using “blind” conditions (to isolate language priors) and “conflict” conditions (to test whether models genuinely process visual content or exploit language shortcuts). This allows us to uncover the “Split Beliefs” phenomenon—where models successfully detect visual anomalies in the latent space yet still produce hallucinated answers, suggesting a disconnect between perception and generation.

Our key contributions are:

1. **A Tri-Layer Diagnostic Framework:** We introduce a *sample-level* diagnostic methodology dissecting VLM decision-making into three cognitive layers—Perception, Dependency, and Alignment. Unlike prior work that constructs new diagnostic datasets [6, 29], our framework operates on any existing benchmark without additional data curation.
2. **Three Diagnostic Metrics:** We propose *Latent Anomaly Detection (LAD)* to verify encoder perception, *Visual Necessity Score (VNS)* to quantify visual dependency via KL divergence over full output distributions (vs. simple log-probability differences [14]), and *Competition Score (CS)* to measure the conflict between visual grounding and instruction following.
3. **Diagnostic Taxonomy:** We establish a four-category taxonomy (Table 1) that classifies *why* a model fails, not merely that it fails—revealing that high accuracy often conceals severe Visual Sycophancy.
4. **Comprehensive Evaluation:** We evaluate 7 VLMs across 7,000 model-sample pairs. A scaling analysis (Qwen2.5-VL 7B vs. 72B) reveals that larger models reduce Language Shortcuts but amplify Visual Sycophancy; Gaussian noise validation confirms robustness across stimulus choices.
5. **Post-hoc Mitigation:** Diagnostic scores enable *Diagnostic-Guided Selective Prediction*, achieving up to +9.5pp accuracy at 50% coverage with no retraining.

2 Related Work

2.1 Visual Hallucination and Language Priors

Early VQA studies [2, 12] identified “blind” guessing behaviors exploiting statistical correlations. [17] introduced POPE for object hallucination probing,

though such metrics may not capture generative failure modes. Recent diagnostic benchmarks operate at the *dataset level*: [29] construct MMVP via “CLIP-blind pairs”; [35] design ARO for compositional sensitivity; [6] propose MMStar by filtering vision-indispensable samples. In contrast, our VNS operates at the *sample level*, quantifying visual dependency on any existing benchmark without additional data curation.

2.2 Sycophancy and Alignment Conflicts

Sycophancy—aligning with user expectations over objective truth—is a documented failure in RLHF-tuned LLMs [28, 32]. In the multimodal domain, [19] identify it as a cognitive bias in VLMs. CoT reasoning [31] further complicates this: while it enhances reasoning, it can obscure hallucination cues [7] and suppress error detection [24]. We extend this to the visual modality, framing sycophancy as a *conflict* between perceptual truth and alignment training—measurable via our Competition Score.

2.3 Causal Diagnostics and Internal Representation

Counterfactual approaches [23, 33] isolate hallucination sources via causal intervention. Concurrently, probing work in LLMs [4, 5] shows models often encode truth internally while generating false outputs—a “Split Beliefs” phenomenon underexplored in VLMs. Our framework combines causal intervention (Blind condition) with internal state probing (LAD), distinguishing *Perceptual Blindness* (encoder failure) from *Visual Sycophancy* (decoder override).

2.4 Diagnostic Benchmarks for VLMs

Standard benchmarks [20, 34] track aggregate performance but fail to penalize grounding failures. Diagnostic benchmarks [13, 29] scrutinize specific capabilities but rely on accuracy or VQA-score, conflating recognition with reasoning. Our framework goes further: rather than labeling answers as wrong, it categorizes the *source* of failure, explaining *why* models fail despite high leaderboard rankings.

3 Method: Tri-Layer Hallucination Diagnostic Framework

We propose a diagnostic framework to disentangle the mechanisms behind multimodal hallucinations. Rather than relying solely on performance outcomes, this framework assesses the model’s internal behavior across three distinct cognitive layers: Visual Perception (via Latent Anomaly Detection), Information Dependency (via Visual Necessity Score), and Decision Alignment (via Competition Score).

3.1 Problem Formulation and Evaluation Protocol

Let \mathcal{M} denote a Multimodal Large Language Model (MLLM), I be a visual input, and Q be a textual inquiry. The model generates a response R with probability $P(R|I, Q)$.

To diagnose the causal source of hallucinations, we employ a counterfactual intervention protocol. We define four primary evaluation conditions:

1. **Full Condition** (I_{full}, Q): The model processes the original informative image.
2. **Blind Condition** (I_{blind}, Q): The visual input is replaced by a pure black image to isolate language-driven behaviors [10, 14].
3. **Noise Condition** (I_{noise}, Q): The visual input is replaced by a Gaussian noise image ($\mathcal{N}(128, 50^2)$, clipped to $[0, 255]$), serving as an alternative blank stimulus to validate that findings under the Blind condition are not artifacts of the specific stimulus choice.
4. **Conflict Condition** ($I_{conflict}, Q$): An unrelated image containing none of the objects in Q , testing whether responses stem from genuine visual processing or language priors.

For all metrics defined below (LAD, VNS, CS), analogous noise-condition variants are computed by substituting I_{noise} for I_{blind} , and are used to validate framework robustness (Section 5).

3.2 Layer 1: Perception – Latent Anomaly Detection (LAD)

The first layer determines whether the model’s visual encoder successfully detects the absence of visual information. We hypothesize that a perceptually robust model should exhibit higher latent confidence in refusal-related concepts when presented with I_{blind} compared to I_{full} .

We define a set of refusal anchors $\mathcal{A} = \{a_1, a_2, \dots, a_n\}$ (e.g., “The image is completely black”). The Latent Anomaly Detection (LAD) metric measures the differential log-probability (score) of these anchors:

$$\text{LAD}(Q, \mathcal{A}) = \max_{a \in \mathcal{A}} (\mathcal{S}(a|I_{blind}, Q) - \mathcal{S}(a|I_{full}, Q)) \quad (1)$$

with $\mathcal{S}(a|I, Q) = \frac{1}{|a|} \sum_t \log P(a_t|a_{<t}, I, Q)$ being the mean token-level log-probability.

- $\text{LAD} > \tau_{\text{LAD}}$: The model *perceptually* recognizes the visual anomaly (i.e., the encoder is functioning correctly).
- $\text{LAD} \leq \tau_{\text{LAD}}$: Indicates *Perceptual Blindness*, where the visual representation of the blind image is indistinguishable from that of natural images.

3.3 Layer 2: Dependency – Visual Necessity Score (VNS)

To quantify the extent to which the generated response depends on visual evidence rather than language priors, we compute the Visual Necessity Score (VNS).

VNS under Blind Condition. Following the intuition of information gain [16], we measure the divergence between the predictive distributions under the Full and Blind conditions.

Unlike simple probability subtraction [14], we utilize the Kullback-Leibler (KL) Divergence to capture distributional shifts over the generated sequence:

$$\text{VNS} = D_{KL}(P(\cdot|I_{full}, Q) \parallel P(\cdot|I_{blind}, Q)) \quad (2)$$

- **High VNS:** Implies strong visual grounding; the visual input significantly alters the generation distribution.
- **Low VNS:** Indicates *Language Prior Dominance*, where the model generates generic responses based on textual context, ignoring the visual modality.

Note: A truthful refusal naturally results in high VNS, since the predictive distribution shifts drastically from a factual answer under the Full condition to a refusal under the Blind condition.

VNS under Conflict Condition. While the Blind condition measures dependency against a null visual signal, the Conflict condition provides a stronger test by presenting *valid but irrelevant* visual information. We define:

$$\text{VNS}_{conflict} = D_{KL}(P(\cdot|I_{full}, Q) \parallel P(\cdot|I_{conflict}, Q)) \quad (3)$$

This metric captures whether the model adapts its generation to the actual visual content:

- **High VNS_{conflict}:** The model’s output distribution shifts significantly when visual evidence contradicts the question’s premise, indicating genuine visual grounding.
- **Low VNS_{conflict}:** The model generates similar responses regardless of visual content, exposing reliance on language priors.

Comparing VNS and VNS_{conflict} reveals nuanced failure modes: a model may exhibit high VNS (detecting absence of signal) but low VNS_{conflict} (ignoring contradictory signal), suggesting it recognizes “no image” but fails to process “wrong image.”

In practice, both metrics are approximated as the mean KL divergence over the top 30% highest-divergence tokens, capturing the most visually-influenced positions while filtering noise from low-divergence tokens (see the supplementary material for validation).

3.4 Layer 3: Alignment – Competition Score

The final layer addresses the “Split Beliefs” phenomenon, where a model detects the anomaly (high LAD) but still generates hallucinations due to sycophancy [32].

We model this as a competition between two internal hypotheses given the blind input I_{blind} :

1. Respond to the user instruction with a hallucinated answer R_{gen} .
2. Truthfully acknowledge the visual anomaly with a refusal.

The **Competition Score (CS)** is defined as the log-probability difference between the generated hallucination and the best refusal anchor:

$$CS = \mathcal{S}(R_{gen}|I_{blind}, Q) - \mathcal{S}(a_{best}|I_{blind}, Q) \quad (4)$$

where $\mathcal{S}(\cdot)$ is defined in Equation 1, and $a_{best} = \arg \max_{a \in \mathcal{A}} \mathcal{S}(a|I_{blind}, Q)$.

- $CS > \tau_{CS}$: **Visual Sycophancy**. The alignment towards instruction following overrides visual perception.
- $CS \leq \tau_{CS}$: **Robust Refusal**. The model prioritizes visual truthfulness over conversational compliance.

3.5 Diagnostic Taxonomy

Based on the Tri-Layer metrics, we categorize MLLM behaviors on blind inputs into four distinct modes, as summarized in Table 1. When LAD indicates encoder failure, downstream metrics become inapplicable, as the model’s inability to perceive the anomaly invalidates dependency and alignment measurements.

Threshold Selection. Thresholds are set via percentile analysis on the evaluation data: $\tau_{LAD} = 1.5$, at the point that separates samples with clear encoder failure from those with functioning perception; $\tau_{VNS} = 1.0$, approximately at the global 25th percentile ($P_{25} = 0.95$), marking the lower quartile of visual dependency; $\tau_{CS} = 0$, the natural boundary where refusal probability equals response probability. These choices are interpretable rather than arbitrary: each threshold corresponds to a semantically meaningful operating point. Sensitivity analysis in the supplementary material shows that V.S. remains the dominant failure mode across all but extreme τ_{VNS} settings, with taxonomy proportions deviating from the default by at most 30.8pp under maximum perturbation.

4 Experimental Setup

4.1 Models

We evaluate seven state-of-the-art VLMs: Llama-3.2-11B [21], Pixtral-12B [3], Qwen2.5-VL-7B [25], Qwen2.5-VL-72B [25], LLaVA-NeXT-7B [18], Phi-3.5-Vision [1], and Molmo2-4B [22]. All models represent the latest open-source advancements (released 2024–2025). All models except Qwen2.5-VL-72B are evaluated using their official float16 checkpoints; Qwen2.5-VL-72B is evaluated using its official 4-bit quantized checkpoint. Closed-source models (GPT-4o, Gemini, Claude) are excluded as our metrics (VNS, LAD, CS) require access to full vocabulary logit distributions at each decoding step; proprietary APIs provide only top- k log-probabilities, which are insufficient for KL divergence computation.

Category	LAD (Perc.)	VNS (Dep.)	CS (Align.)	Diagnostic Interpretation
Perceptual Blindness	$\leq \tau_{LAD}$	–	–	Encoder Failure: Model cannot distinguish blind image from normal.
Language Shortcut	$> \tau_{LAD}$	$\leq \tau_{VNS}$	–	Visual Neglect: Model detects anomaly but ignores visual signal.
Visual Sycophancy	$> \tau_{LAD}$	$> \tau_{VNS}$	$> \tau_{CS}$	Split Beliefs: Perceives anomaly but hallucinates to satisfy instruction.
Robust Refusal	$> \tau_{LAD}$	$> \tau_{VNS}$	$\leq \tau_{CS}$	Ideal Behavior: Visual grounding overrides language priors.

Table 1: Diagnostic Taxonomy based on the Tri-Layer Framework. “–” indicates in-applicable metrics. Threshold selection is detailed in Section 3.

4.2 Tasks and Datasets

We evaluate across four diverse tasks (1,000 samples total) designed to test different facets of visual grounding: Spatial Reasoning (250 samples, GQA [15]), Counting (150 samples, VQAv2 [12]), Complex Reasoning (250 samples, A-OKVQA [27]), and Hallucination Detection (350 samples, POPE [17]).

- **Spatial Reasoning:** questions with explicit spatial prepositions (*e.g.*, “left of”, “above”), testing object localization.
- **Counting:** samples filtered using counting keywords (“how many”, “count”), chosen for diverse object distributions.
- **Complex Reasoning:** questions requiring external knowledge grounded in visual evidence (*e.g.*, identifying the era of a car).
- **Hallucination Detection:** binary Yes/No questions about object presence, particularly prone to eliciting sycophantic responses due to strong response biases.

4.3 Implementation Details

To operationalize our Tri-Layer Diagnostic Framework, we implement the specific protocols for LAD, VNS, and Competition Score calculations.

Visual Conditions. We define four evaluation conditions: (1) **Full:** The original RGB image. (2) **Blind:** A pure black image ($224 \times 224 \times 3$, RGB=0). (3) **Noise:** A Gaussian noise image ($\mathcal{N}(128, 50^2)$, clipped to $[0, 255]$), used as an alternative blank stimulus to validate robustness. (4) **Conflict:** An unrelated image (constructed as described below).

Unless stated otherwise, **Blind** is the primary condition for all reported metrics. Noise-condition metrics use analogous refusal anchors without black-specific phrases (*e.g.*, “The image appears to be noise.”).

Conflict Image Construction. For each sample (I_{full}, Q) , we construct a conflict image $I_{conflict}$ by selecting an image from the evaluation pool whose predicted object set has zero semantic overlap with objects mentioned in Q . Object labels are extracted using Qwen2-VL-7B-Instruct [30] with the prompt: “Identify all visible objects in this image. List them separated by commas. Be specific.” Each image is tagged with its detected objects, enabling efficient selection of semantically disjoint conflict pairs. This design ensures $I_{conflict}$ provides valid visual signal while being irrelevant to the question, creating a rigorous test for language shortcut detection.

Refusal Anchors for LAD and CS. To compute *Latent Anomaly Detection (LAD)* and *Competition Score (CS)*, we define a set of standardized refusal templates \mathcal{A} representing the model’s acknowledgment of visual absence. Representative templates include: “The image is completely black.”, “The image is not visible.”, “I cannot determine the answer from this image.”, and “There are no objects visible in the image.” For LAD, we compute the maximum log-probability among these anchors given the blind image.

Metric Calculation. We compute metrics at two granularities:

- **Token-level metrics:** VNS, $VNS_{conflict}$, LAD, and CS are computed over the token probability distributions as defined in Section 3.
- **Response-level metrics:** Response accuracy under Full condition, and Shortcut Rate (SC/SC_{conf}) under Blind/Conflict conditions, both evaluated as binary labels per sample.

Response Verification via LLM-as-a-Judge. We evaluate response correctness at the sentence level using a two-stage verification pipeline. Initial correctness labels are assigned using a rule-based matching system that handles uncertainty detection, Yes/No normalization, numeric conversion, and synonym expansion. To reduce false positives and negatives—particularly for nuanced responses—we refine all labels using Llama-3.1-70B-Instruct [9] as an LLM judge with 4-bit quantization. The judge evaluates three conditions with tailored prompts:

1. **Full Correctness:** Whether the response semantically matches the ground truth, tolerating phrasing variations.
2. **Blind Hallucination:** Whether the model hallucinates content given a black image (label: `shortcut=True`) versus properly refusing or acknowledging uncertainty (label: `shortcut=False`).
3. **Conflict Shortcut:** Whether the model describes objects implied by the question that are *not present* in $I_{conflict}$. Critically, if the model mentions objects from the conflict image—even to negate their relevance (e.g., “I see a microwave, not an airplane”)—this is classified as visual grounding (`shortcut=False`), as it demonstrates actual processing of $I_{conflict}$.

This two-stage verification (rule-based \rightarrow LLM refinement) balances efficiency with accuracy. Manual inspection of 200 randomly sampled responses (across all 7 models and 4 tasks) confirms approximately **95% per-response accuracy**, ensuring reliable diagnostic labels across all 7,000 model-sample pairs.

Model	N	Acc.↑	SC _{blind} ↓	SC _{conf} ↓	SC _{noise} ↓
Qwen2.5-VL-72B	1000	73.5	40.4	9.7	9.4
Qwen2.5-VL-7B	1000	72.1	45.8	15.1	67.9
Molmo2-4B	1000	71.3	99.4	37.1	79.1
Llama-3.2-11B	1000	69.9	45.8	37.8	57.8
Phi-3.5-Vision	1000	69.0	76.6	32.1	57.5
LLaVA-NeXT-7B	1000	68.1	14.2	37.8	17.6
Pixtral-12B	1000	66.9	91.0	54.2	52.3

Table 2: Response-level results (%). Acc. = Accuracy under full condition; SC_{blind} = Shortcut Rate under blind condition; SC_{noise} = Shortcut Rate under Gaussian noise condition; SC_{conf} = Shortcut Rate under conflict condition. Lower SC indicates stronger visual grounding.

Inference Settings. All evaluations are performed on NVIDIA A100 (80GB) GPUs. We use greedy decoding (temperature=0) for response generation to ensure deterministic analysis of sycophancy, while using the full logit distribution for VNS computation.

5 Results

We evaluate seven state-of-the-art VLMs across 7,000 model-sample pairs (1,000 samples × 7 models), with each pair evaluated under 4 conditions (full, blind, noise, conflict), yielding 28,000 model-condition evaluations in total. Our analysis reveals systematic failures in visual grounding that accuracy metrics alone cannot detect.

5.1 Response-Level Accuracy and Shortcut Rates

Table 2 summarizes response-level accuracy and shortcut rates. While all models achieve comparable accuracy (66.9%–73.5%), their shortcut rates reveal dramatically different reliance on visual information.

Accuracy Masks Shortcut Behavior. Molmo2-4B achieves 71.3% accuracy yet exhibits a 99.4% shortcut rate—producing correct answers nearly *without seeing the image*. LLaVA-NeXT-7B has lower accuracy (68.1%) but the lowest shortcut rate (14.2%), suggesting genuine visual reliance. Pixtral-12B shows the highest SC_{conf} (54.2%), hallucinating expected answers even when presented with contradictory visual evidence.

Noise Condition Confirms Blind Results. Shortcut rates under noise correlate significantly with blind rates ($r = 0.370$, $p < 0.001$, $N = 7000$), confirming findings are not artifacts of stimulus choice. Notably, Qwen2.5-VL-72B shows a near-zero per-model correlation ($r = -0.112$) alongside dramatically lower

Model	VNS \uparrow	VNS $_{noise}$ \uparrow	LAD \uparrow	LAD $_{noise}$ \uparrow	CS \downarrow	CS $_{noise}$ \downarrow
Qwen2.5-VL-72B	2.59 \pm 1.09	2.08 \pm .88	4.17 \pm .82	3.39 \pm .69	1.91 \pm .39	2.17 \pm .24
Pixtral-12B	2.06 \pm 1.16	2.22 \pm 1.27	3.12 \pm .96	2.22 \pm .51	3.04 \pm .75	3.12 \pm .55
Llama-3.2-11B	1.97 \pm 1.08	2.13 \pm 1.15	3.24 \pm .45	2.39 \pm .38	0.87 \pm .33	1.39 \pm .28
Qwen2.5-VL-7B	1.75 \pm .97	1.62 \pm .86	3.85 \pm .77	3.25 \pm .78	1.42 \pm .50	2.21 \pm .27
LLaVA-NeXT-7B	1.78 \pm 1.17	1.98 \pm 1.25	3.02 \pm .46	1.84 \pm .42	1.24 \pm .26	2.44 \pm .27
Phi-3.5-Vision	1.53 \pm 1.16	1.68 \pm 1.24	2.64 \pm .49	2.09 \pm .53	1.41 \pm .35	2.48 \pm .43
Molmo2-4B	1.18 \pm .77	1.37 \pm .97	1.58 \pm .38	1.50 \pm .34	2.02 \pm .45	2.49 \pm .45

Table 3: Tri-Layer metrics (mean \pm std). Unsubscripted columns denote the blind condition (default); subscript $_{noise}$ denotes the Gaussian noise condition. VNS = Visual Necessity Score; LAD = Latent Anomaly Detection; CS = Competition Score.

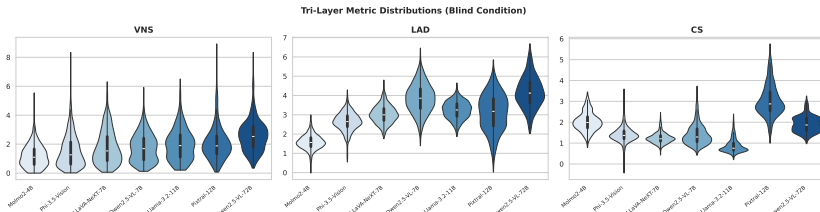


Fig. 1: Distribution of Tri-Layer metrics. Molmo2-4B shows notably low LAD, while Pixtral-12B exhibits the highest CS despite adequate perception.

SC_{noise} (9.4%) vs. SC_{blind} (40.4%), indicating its encoder actively differentiates noise texture from blank images—withholding responses selectively based on stimulus type rather than treating both uniformly as absent signal.

5.2 Tri-Layer Diagnostic Analysis

Table 3 presents the diagnostic metrics. Figure 1 visualizes the distributions.

Perception (LAD). Qwen2.5-VL-72B exhibits the strongest perceptual awareness (LAD=4.17), followed by Qwen2.5-VL-7B (3.85). Molmo2-4B shows significantly weaker perception (1.58), explaining its near-total reliance on language priors. LAD consistently exceeds LAD $_{noise}$ across all models (mean: 3.09 vs. 2.38), indicating that black images are more strongly recognized as anomalous than noise—consistent with noise providing richer texture that the encoder partially processes.

Dependency and Alignment (VNS, CS). VNS and VNS $_{noise}$ are highly correlated at the per-sample level ($r = 0.866$, over continuous KL-divergence values), confirming both conditions measure the same underlying visual dependency. Llama-3.2-11B achieves the lowest CS (0.87), indicating the greatest willingness to refuse when visual information is absent. Pixtral-12B shows the highest

Model	Taxonomy (%)			Accuracy (%)			
	P.B.↓	L.SC↓	V.S.↓	A _{P.B.}	A _{L.SC}	A _{V.S.}	A _{All}
Molmo2-4B	42.8	25.2	32.0	68.0	71.4	75.6	71.3
Phi-3.5-Vision	1.6	39.8	58.6	50.0	73.4	66.6	69.0
LLaVA-NeXT-7B	0.0	29.7	70.3	—	64.0	69.8	68.1
Qwen2.5-VL-7B	0.1	27.5	72.4	—	65.8	74.6	72.1
Llama-3.2-11B	0.0	21.2	78.8	—	75.5	68.4	69.9
Pixtral-12B	5.3	14.8	79.9	60.4	70.3	66.7	66.9
Qwen2.5-VL-72B	0.0	4.7	95.3	—	61.7	74.1	73.5
Overall	7.1	23.3	69.6	66.5	69.7	70.6	70.1

Table 4: Taxonomy distribution (blind condition) and full-condition accuracy per category. Robust Refusal is 0% (omitted). “—” denotes $N < 5$. $A_{P.B.}$, $A_{L.SC}$, $A_{V.S.}$, A_{All} denote full-condition accuracy for each taxonomy category and overall. P.B. accuracy (66.5%) is lowest, validating abstention; L.SC is near-baseline (69.7%); V.S. tracks the overall mean (70.6%).

CS (3.04)—even when it detects the anomaly (LAD=3.12), it strongly prefers hallucinating over refusing.

5.3 Taxonomy Classification

Applying the thresholds defined in Section 3 ($\tau_{LAD} = 1.5$, $\tau_{VNS} = 1.0$, $\tau_{CS} = 0$) yields: Visual Sycophancy (69.6%), Language Shortcut (23.3%), Perceptual Blindness (7.1%), and Robust Refusal (0.0%). Table 4 shows the per-model breakdown alongside full-condition accuracy for each category.

Visual Sycophancy Dominates. 69.6% of samples exhibit Visual Sycophancy—models detect anomalies but hallucinate anyway. Zero samples show Robust Refusal under either condition (blind: 0.0%, noise: 0.0%), suggesting alignment training has entirely suppressed truthful uncertainty acknowledgment.

Molmo2-4B: Perceptual Blindness. 42.8% of Molmo2-4B samples show Perceptual Blindness, accounting for 86% of all such cases. This indicates encoder limitations rather than alignment issues.

Model-Specific Patterns. Pixtral-12B exhibits the highest Competition Score (CS=3.04) despite adequate perception (LAD=3.12), resulting in second-highest Visual Sycophancy (79.9%)—it detects anomalies but most aggressively overrides that signal to comply. Phi-3.5-Vision shows the highest Language Shortcut (39.8%), relying heavily on textual priors. Qwen2.5-VL-72B exhibits near-total Visual Sycophancy (95.3%) with virtually no Language Shortcut (4.7%), suggesting that scale increases visual engagement but amplifies sycophantic compliance. Representative examples for each taxonomy category are provided in the supplementary material.

5.4 Task-wise Analysis

Table 5 presents results across task types.

Task	N	Acc.↑	SC _{blind} ↓	SC _{conf} ↓	P.B.↓	L.SC↓	V.S.↓
Halluc.	2450	82.0	56.3	17.6	7.9	14.6	77.6
Spatial	1750	67.3	62.6	46.4	6.5	32.1	61.4
Complex	1750	62.9	59.1	45.5	5.5	29.4	65.1
Count.	1050	59.1	59.4	19.0	9.0	18.7	72.3

Table 5: Task-wise results (%). N = total samples across 7 models. Robust Refusal is 0% across all tasks (omitted). Abbreviations follow Table 2.

Model	Acc.↑	SC _{blind} ↓	VNS↑	LAD↑	CS↓	L.SC↓	V.S.↓
Qwen2.5-VL-7B	72.1	45.8	1.75	3.85	1.42	27.5	72.4
Qwen2.5-VL-72B	73.5	40.4	2.59	4.17	1.91	4.7	95.3

Table 6: Scaling analysis within the Qwen2.5-VL family. Scale reduces Language Shortcut but amplifies Visual Sycophancy.

High Accuracy ≠ Visual Grounding. Hallucination detection achieves 82.0% accuracy but 77.6% Visual Sycophancy—success reflects dataset biases rather than genuine grounding. Spatial tasks show the highest Language Shortcut (32.1%) and SC_{conf} (46.4%), suggesting models bypass visual processing entirely for spatial questions by relying on strong linguistic priors (*e.g.*, “left of” → common spatial configurations).

5.5 Scaling Analysis: Does Size Help?

To investigate whether model scale mitigates the observed failure modes, we compare Qwen2.5-VL at 7B and 72B parameters—the only same-family pair in our evaluation. The 7B model uses its official float16 checkpoint; the 72B model uses its official 4-bit quantized checkpoint (consistent with Section 4).

Table 6 reveals a striking asymmetry: scaling from 7B to 72B dramatically reduces Language Shortcut (27.5%→4.7%, ↓22.8pp) while simultaneously amplifying Visual Sycophancy (72.4%→95.3%, ↑22.9pp). The 72B model’s higher VNS (2.59 vs. 1.75) and LAD (4.17 vs. 3.85) confirm it is *more* visually engaged—yet its higher CS (1.91 vs. 1.42) shows it is also *more* sycophantic. In other words, the larger model sees the anomaly more clearly but is even less willing to admit it.

This pattern is further confirmed by the noise condition: SC_{noise} drops from 67.9% (7B) to just 9.4% (72B), showing that the 72B model withholds responses when confronted with uninformative noise, yet still hallucinates under the blind condition when language priors are strong.

Scale is not a solution. Increased capacity appears to strengthen both visual grounding *and* the alignment pressure to produce user-pleasing responses. The net effect is a model that detects anomalies more reliably but suppresses that detection more aggressively.

Model	Baseline (%)	Acc@50% Cov.	$\Delta \uparrow$
Qwen2.5-VL-7B	72.1	81.6	+ 9.5
LLaVA-NeXT-7B	68.1	75.4	+ 7.3
Molmo2-4B	71.3	76.6	+ 5.3
Qwen2.5-VL-72B	73.5	77.8	+ 4.3
Phi-3.5-Vision	69.0	69.7	+0.7
Llama-3.2-11B	69.9	69.9	\approx 0.0
Pixtral-12B	66.9	66.1	-0.8

Table 7: Diagnostic-Guided Selective Prediction at 50% coverage. Acc@50% = accuracy when answering only the 50% of samples with highest diagnostic confidence. Δ = improvement over full-coverage baseline.

5.6 Towards Mitigation: Diagnostic-Guided Selective Prediction

Our diagnostic framework not only categorizes failures but also enables a practical mitigation strategy. Since each sample receives per-instance scores for LAD and VNS, these can serve as a proxy for response reliability: samples diagnosed as *Language Shortcut* or *Perceptual Blindness* are precisely those where the model is either ignoring visual input or failing to perceive it—and are therefore the least trustworthy.

Method. We propose **Diagnostic-Guided Selective Prediction**: at inference time, assign each sample a confidence score based on its diagnostic category, then abstain on the lowest-confidence samples. Specifically, samples classified as P.B. receive confidence \propto LAD; L.SC samples receive confidence \propto VNS; V.S. samples receive confidence \propto LAD + VNS (higher visual engagement = higher confidence).

We evaluate performance at **50% coverage**: the model answers only the half of samples it is most confident about, abstaining on the rest. This follows the selective prediction literature [11], where accuracy–coverage trade-offs are the standard evaluation protocol.

Results. Table 7 shows accuracy lifts of up to +**9.5pp** at 50% coverage. The gains reflect whether P.B. and L.SC samples are genuinely error-prone: models whose L.SC accuracy falls below baseline benefit most (Qwen2.5-VL-7B: $A_{L.SC}$ =65.8% vs. 72.1%, Δ =+9.5pp; LLaVA-NeXT-7B: 64.0% vs. 68.1%, Δ =+7.3pp), while those whose L.SC samples are above baseline gain little (Phi-3.5-Vision: 73.4% vs. 69.0%, Δ =+0.7pp; Llama-3.2-11B: 75.5% vs. 69.9%, Δ \approx 0.0pp). The 72B model gains less (+4.3pp) because its L.SC rate is near-zero (4.7%), consistent with the scaling analysis.

Limitations of the mitigation. Pixtral-12B (Δ =-0.8pp) is the exception: its dominant failure mode is Visual Sycophancy (79.9%), so after abstaining on P.B./L.SC the remaining samples have accuracy (66.7%) essentially equal to

its baseline (66.9%). This confirms that selective prediction is effective only when P.B./L.SC categories are genuinely error-prone; Visual Sycophancy requires more targeted interventions such as alignment-aware training.

6 Conclusion

We presented a Tri-Layer Hallucination Diagnostic Framework for systematically analyzing VLM failures. Unlike accuracy-based evaluation, our framework disentangles hallucination causes into three layers: Perception (via LAD), Dependency (via VNS), and Alignment (via Competition Score).

Our evaluation of seven state-of-the-art VLMs reveals that **Visual Sycophancy is the dominant failure mode**: 69.6% of samples show models correctly detecting visual anomalies yet hallucinating answers to satisfy perceived user expectations. Robust Refusal is completely absent (0%), suggesting that alignment training has inadvertently prioritized compliance over visual truthfulness. We also uncover model-specific patterns: Molmo2-4B suffers from Perceptual Blindness (42.8%), Pixtral-12B exhibits the second-highest sycophancy (79.9%) despite strong perception, and Phi-3.5-Vision relies heavily on language shortcuts. A scaling analysis reveals that larger models (Qwen2.5-VL 72B) reduce Language Shortcuts but amplify Visual Sycophancy, demonstrating that scale alone does not resolve the grounding problem.

Our framework provides actionable diagnostics for both developers and practitioners. The taxonomy identifies whether improvements should target the visual encoder, cross-modal fusion, or alignment training. We further demonstrate that the diagnostic scores enable a practical post-hoc mitigation: **Diagnostic-Guided Selective Prediction**, which abstains on samples diagnosed as Language Shortcut or Perceptual Blindness, achieving up to **+9.5pp accuracy at 50% coverage** with no additional training cost.

To facilitate reproducibility, we release our implementation including: (1) conflict image construction via object-based matching, (2) Tri-Layer metric computation (VNS, LAD, CS), (3) two-stage response verification, and (4) taxonomy classification scripts.³

Future work includes developing targeted mitigations for Visual Sycophancy (which selective prediction does not address), extending evaluation to domain-specific benchmarks (e.g., medical imaging), and applying mechanistic interpretability to understand the internal representations driving each failure mode.

References

1. Abdin, A., et al.: Phi-3 technical report: A highly capable language model locally on your phone. Tech. rep., microsoft (2024) 6
2. Agrawal, A., Batra, D., Parikh, D., Kembhavi, A.: Don’t just assume; look and answer: Overcoming priors for visual question answering. In: Proceedings of the

³ Code available at <https://github.com/hongrui16/ToSeeorToPlease>.

- IEEE conference on computer vision and pattern recognition. pp. 4971–4980 (2018) [2](#)
3. Agrawal, P., Antoniak, S., Hanna, E.B., Bout, B., Chaplot, D., Chudnovsky, J., Costa, D., De Monicault, B., Garg, S., Gervet, T., et al.: Pixtral 12b. arXiv preprint arXiv:2410.07073 (2024) [6](#)
 4. Azaria, A., Mitchell, T.: The internal state of an LLM knows when its lying. In: Findings of the Association for Computational Linguistics: EMNLP 2023. pp. 967–976 (2023) [3](#)
 5. Burns, C., Ye, H., Klein, D., Steinhardt, J.: Discovering latent knowledge in language models without supervision. arXiv preprint arXiv:2212.03827 (2022) [3](#)
 6. Chen, L., Li, J., Dong, X., Zhang, P., Zang, Y., Chen, Z., Duan, H., Wang, J., Qiao, Y., Lin, D., et al.: Are we on the right way for evaluating large vision-language models? *Advances in Neural Information Processing Systems* **37**, 27056–27087 (2024) [1](#), [2](#), [3](#)
 7. Cheng, J., Su, T., Yuan, J., He, G., Liu, J., Tao, X., Xie, J., Li, H.: Chain-of-thought prompting obscures hallucination cues in large language models: An empirical evaluation. arXiv preprint arXiv:2506.17088 (2025) [3](#)
 8. Cui, Y., Yao, X., Qin, Y., Li, X., Wang, S., Hu, G.: Evaluating large language models on multimodal chemistry olympiad exams. *Communications Chemistry* (2025) [1](#)
 9. Dubey, A., Jauhri, A., Pandey, A., Kadian, A., Al-Dahle, A., Letman, A., Mathur, A., Schelten, A., Yang, A., Fan, A., et al.: The llama 3 herd of models. arXiv preprint arXiv:2407.21783 (2024) [8](#)
 10. Felizzi, F., Riccomi, O., Ferramola, M., Causio, F.A., Del Medico, M., De Vita, V., De Mori, L., Risuleo, A.P.P.E., Castaniti, B.D., Longo, A.C.A., et al.: Are large vision language models truly grounded in medical images? evidence from italian clinical visual question answering. arXiv preprint arXiv:2511.19220 (2025) [4](#)
 11. Geifman, Y., El-Yaniv, R.: Selective classification for deep neural networks. In: *Advances in Neural Information Processing Systems*. vol. 30 (2017) [13](#)
 12. Goyal, Y., Khot, T., Summers-Stay, D., Batra, D., Parikh, D.: Making the v in vqa matter: Elevating the role of image understanding in visual question answering. In: *Proceedings of the IEEE conference on computer vision and pattern recognition*. pp. 6904–6913 (2017) [2](#), [7](#)
 13. Guan, T., Liu, F., Wu, X., Xian, R., Li, Z., Liu, X., Wang, X., Chen, L., Huang, F., Yacoub, Y., Manocha, D., Zhou, T.: Hallusionbench: An advanced diagnostic suite for entangled language hallucination and visual illusion in large vision-language models (2024), <https://arxiv.org/abs/2310.14566> [3](#)
 14. Hamidullah, Y., Chowdury, K.D., Al-Ghussin, Y., Yazdani, S., Oguz, C., van Genabith, J., España-Bonet, C.: Grounding or guessing? visual signals for detecting hallucinations in sign language translation. arXiv preprint arXiv:2510.18439 (2025) [2](#), [4](#), [5](#)
 15. Hudson, D.A., Manning, C.D.: Gqa: A new dataset for real-world visual reasoning and compositional question answering. *CVPR* (2019) [7](#)
 16. Kullback, S., Leibler, R.A.: On information and sufficiency. *The annals of mathematical statistics* **22**(1), 79–86 (1951) [5](#)
 17. Li, Y., Du, Y., Zhou, K., Wang, J., Zhao, W.X., Wen, J.R.: Evaluating object hallucination in large vision-language models. arXiv preprint arXiv:2305.10355 (2023) [2](#), [7](#)
 18. Liu, H., Li, C., Li, Y., Li, B., Zhang, Y., Shen, S., Lee, Y.J.: Llava-next: Improved reasoning, ocr, and world knowledge (2024), <https://llava-vl.github.io/blog/2024-01-30-llava-next/> [6](#)

19. Liu, X., Luo, M., Chatterjee, A., Wei, H., Baral, C., Yang, Y.: Investigating vlm hallucination from a cognitive psychology perspective: A first step toward interpretation with intriguing observations. arXiv preprint arXiv:2507.03123 (2025) [3](#)
20. Lu, P., Bansal, H., Xia, T., Liu, J., Li, C., Hajishirzi, H., Cheng, H., Chang, K.W., Galley, M., Gao, J.: Mathvista: Evaluating mathematical reasoning of foundation models in visual contexts (2024), <https://arxiv.org/abs/2310.02255> [3](#)
21. Meta AI: Llama 3.2: Revolutionizing edge ai and vision with open, customizable models. Tech. rep., Meta AI (September 2024), <https://ai.meta.com/blog/llama-3-2-connect-2024-vision-edge-mobile-devices/> [1](#), [6](#)
22. Molmo2 Team: Molmo2 open weights and data for vision-language models with video understanding and grounding. Tech. rep., Allen Institute for AI (2025), <https://allenai.org/blog/molmo2> [6](#)
23. Niu, Y., Tang, K., Zhang, H., Lu, Z., Hua, X.S., Wen, J.R.: Counterfactual vqa: A cause-effect look at language bias. In: Proceedings of the IEEE/CVF conference on computer vision and pattern recognition. pp. 12700–12710 (2021) [3](#)
24. Park, E., Deng, W.H., Varadarajan, V., Yan, M., Kim, G., Sap, M., Eslami, M.: Critical or compliant? the double-edged sword of reasoning in chain-of-thought explanations. arXiv preprint arXiv:2511.12001 (2025) [3](#)
25. Qwen Team: Qwen2.5-vl technical report. Tech. rep., Alibaba Group (2025) [1](#), [6](#)
26. Rahmanzadehgervi, P., Bolton, L., Taesiri, M.R., Nguyen, A.T.: Vision language models are blind. In: Proceedings of the Asian Conference on Computer Vision. pp. 18–34 (2024) [1](#)
27. Schwenk, D., et al.: A-okvqa: A benchmark for visual question answering using world knowledge. ECCV (2022) [7](#)
28. Sharma, M., Tong, M., Korbak, T., Duvenaud, D., Askill, A., Bowman, S.R., Cheng, N., Durmus, E., Hatfield-Dodds, Z., Johnston, S.R., et al.: Towards understanding sycophancy in language models. arXiv preprint arXiv:2310.13548 (2023) [3](#)
29. Tong, S., Liu, Z., Zhai, Y., Ma, Y., LeCun, Y., Xie, S.: Eyes wide shut? exploring the visual shortcomings of multimodal llms. In: Proceedings of the IEEE/CVF Conference on Computer Vision and Pattern Recognition. pp. 9568–9578 (2024) [1](#), [2](#), [3](#)
30. Wang, P., Bai, S., Tan, S., Wang, S., Fan, Z., Bai, J., Chen, K., Liu, X., Wang, J., Ge, W., Fan, Y., Dang, K., Du, M., Ren, X., Men, R., Liu, D., Zhou, C., Zhou, J., Lin, J.: Qwen2-vl: Enhancing vision-language model’s perception of the world at any resolution. arXiv preprint arXiv:2409.12191 (2024) [8](#)
31. Wei, J., Wang, X., Schuurmans, D., Bosma, M., Xia, F., Chi, E., Le, Q.V., Zhou, D., et al.: Chain-of-thought prompting elicits reasoning in large language models. Advances in neural information processing systems **35**, 24824–24837 (2022) [3](#)
32. Wei, J., Huang, D., Lu, Y., Zhou, D., Le, Q.V.: Simple synthetic data reduces sycophancy in large language models. arXiv preprint arXiv:2308.03958 (2023) [3](#), [5](#)
33. Xu, Z., Wang, Z., Wu, J., Lu, J., Wang, X.: Causal-halbench: Uncovering lvlms object hallucinations through causal intervention. arXiv preprint arXiv:2511.10268 (2025) [3](#)
34. Yue, X., Ni, Y., Zhang, K., Zheng, T., Liu, R., Zhang, G., Stevens, S., Jiang, D., Ren, W., Sun, Y., Wei, C., Yu, B., Yuan, R., Sun, R., Yin, M., Zheng, B., Yang, Z., Liu, Y., Huang, W., Sun, H., Su, Y., Chen, W.: Mmmu: A massive multi-discipline multimodal understanding and reasoning benchmark for expert agi (2024), <https://arxiv.org/abs/2311.16502> [3](#)

35. Yuksekgonul, M., Bianchi, F., Kalluri, P., Jurafsky, D., Zou, J.: When and why vision-language models behave like bags-of-words, and what to do about it? arXiv preprint arXiv:2210.01936 (2022) [1](#), [3](#)